Vision Towards 5G: Comparison of Radio Propagation Models for Licensed and Unlicensed Indoor Femtocell Sensor Networks

Noman Shabbir[1], Lauri Kütt[1], Muhammad. M. Alam[2], Priit Rossipuu[2], Muhammad Jawad[3], Muhammad B. Qureshi[3], Ali R. Ansari[4], and Raheel Nawaz[5]

[1] Dept. of Electrical Power Engineering & Mechatronics, Tallinn University of Technology, Estonia;
[2] Thomas Johann Seebeck Institute of Electronics, Tallinn University of Technology, Estonia;
[3] Dept. of Electrical and Computer Engineering, COMSATS University Islamabad, Pakistan;
[4] Gulf University of Science and Technology, Kuwait City, Kuwait;
[5] Manchester Metropolitan University (MMU), Manchester, United Kingdom
* Correspondence: noshab@taltech.ee;

Abstract: Sensors and sensor networks are the future of fully automated industry solutions. With more capability and complex machinery, the requirements for sensing in larger factories are critical, considering the data amount, latency, and the number of sensors in operation. Given the excellent time-critical operation, bandwidth and the number of devices connected, the 5G indoor femtocells could prove an excellent option for building industrial sensor grids. For more flexibility in control and reliability, operating the 5G indoor femtocell network in license-free frequency bands could be an alternative to commercial 5G services. The 5G networks incorporate a very dense network of indoor femtocells. The Femtocells also enhance data rates, indoor performance, and coverage area both in residential and industrial environments. Therefore, keeping in view the above-stated actualities, this paper addresses different indoor scenarios for radio wave propagation and simulates several path loss models to calculate the likely and most suitable propagation model for indoor signaling. Multiple models for frequencies in the unlicensed band below 6 GHz and above 6 GHz (licensed) 5G femtocells are discussed in the paper considering the constraints of material types, attenuation due to obstacles, various floors, carrier frequency, and distance from the transmitter. The comparative analysis indicates that the ITU model and Keenan-Motley model give the highest path loss in residential and industrial environments, respectively, while the log-distance model has the lowest path loss in both environments for below 6 GHz frequencies in the unlicensed spectrum. For the above 6 GHz licensed bands, the Alpha Beta Gamma (ABG) model and Path Loss Exponent (CIF) model are observed to have the minimum path loss difference.

Keywords: 5G; Radio Propagation Models; Femtocells; Indoor Communication; Unlicensed band;

1. Introduction

Telecommunication is one of the fastest growing industries in the world. The increased usage of mobile devices and the demand for higher capacity in modern networks is growing each year. According to a conservative estimate, the number of connected devices will be higher than 20 billion by the end of 2025 [1]–[3]. With the advancements in wireless technology, standards have been defined to overcome the issue of demand and capacity [4], [5]. Modern users require bigger and faster data services; therefore, requiring larger amounts of bandwidth. Due to wider bandwidth demands, mobile networks are struggling to compete with fixed internet connections based on data rates. All this is making the cornerstones for the evolution of wireless networks towards 5th generation (5G) mobile services [6], [7].

The 5G is an upcoming technology intended to provide any type of service, anywhere and anytime [8], [9]. The proposed data rates of 5G are up to 50x (1 Gbps at the cell edge and 10+ Gbps in other areas) with 10x latency improvement and reductions in energy and cost similar to those of the previous generations [10]–[13]. The 5G will be an evolution of the existing Long Term Evolution (LTE) systems [14], [15]. Moreover, the network developer needs to make the current wireless technologies more spectrally efficient along with finding requirements to cover additional capacity and needs [16]–[18]. The 5G's cloud-based service includes not only a move towards the millimeter-wave frequency spectrum but also can give way to completely new bandwidth allocation and reallocation methods based on market data, which can become a major change in the core network [19], [20]. Therefore, a great number of frequency ranges that were never utilized or are underutilized in the spectrum available are urging mobile operators to consider different coexistence options with LTE and come up with new ways for mobile network communications [21], [22]. Nevertheless, the evolution of LTE in unlicensed bands will increase the non-regularity in several data communication technologies, including Wi-Fi, connectivity and disrupt operations [23]. The frequency bands selected by the International Telecommunication Union (ITU) for 5G deployment are shown in Table I [10], [24].

Table I. Proposed frequency bands for 5G

Frequency Band	**Comment**
2.4 GHz	20 to 100 MHz bandwidth (Unlicensed band)
5 GHz	600 MHz bandwidth (Unlicensed band)
24.25 – 27.5 GHz	50 to 400 MHz bandwidth
37.5 – 43.5 GHz	50 to 400 MHz bandwidth
45.5 – 48.2 GHz	Excluding 47 – 47.2 GHz
60 GHZ	7 GHz bandwidth (Unlicensed band)
66-71 GHz	For backhauling
Existing allocated bands	Can be exploited for further efficiency

In order to provide the highest benefit for wireless sensor networks, reliable coverage and availability are vital. The sensors would need to have sufficient link quality, which is a challenge especially keeping in mind the 24 hours availability and low-latency requirements for these networks [25]. Link budget assessment is critical, and all sensors connected should have a healthy overhead for unwanted or unforeseen aspects that might disrupt the sensor data link quality [26]. The propagation characteristics of such networks, especially link loss, would need to be considered and reviewed carefully. Loss of sight, walls in between and the location of nodes on different floors all create additional complexity in establishing sensor network layout planning, selection of equipment, and components [27]. This paper will focus on different models for the assessment of 5G femtocell propagation losses in different industrial and commercial environments, to aid in the planning, placement, and selection of the proper equipment required.

Femtocells offer a completely easy and simple solution to the problem of high bandwidth demand and better coverage [23]. Since femtocells are installed indoors, they are proposed to improve the 5G mobile services coverage in indoor proximity. Furthermore, using unlicensed band femtocells could not only reduce the load on macrocells in urban areas but provide potentially additional network capacity [28], [29]. While they use different radio resources than macrocells; therefore, no interference is seen. It is a very compressed device referred to as Femto access points (FAPs) or home-enhanced eNodeB, the same as used in the 4th Generation (4G). FAPs are installed inside shopping malls, dense towns, plazas, and faraway rural areas [30], [31]. Femtocells are operative on all frequency spectrum ranges covered by 3GPP. However, different service providers can use specific frequency ranges that are distinctively available or more convenient for them [32]. The main control of power for femtocells is discussed in [23], the decentralized methods of femtocells and their pros and cons are discussed in [27], and different techniques regarding the coverage area of femtocells and

their optimization are addressed in [26]. In [33], the authors report that there might be some signal losses based on the strength of nearby macrocell users in the base station and femtocells. In [34], another effective technique used for partitioning is introduced that restricts the FAP to receive anything on the downlink level assigned to the macrocells users.

Numerous studies have focused solely on modifying or creating new indoor propagation models using picocells and femtocells to increase the data rates for indoor users. For instance, in [35], [36], the authors show the experience of the evolution of 3rd Generation Partnership project (3GPP) in the long term at a high level. The Heterogeneous Networks (HetNets) also used several intersymbol interference methods that are crucial. Moreover, in [37], several similar methods are discussed that allow the shifting from macrocells to femtocells, such shifting can also result in increased interference and enhanced coverage of the network. Major efforts were made in enhancing the intercell coordination associated with 3GPP using different research methods and their applications along with the merits [38].

Studies have been done for the path loss estimation of different models concerning 5G networks and test its accuracy and other parameters for large-scale networks [39]–[41]. Radio propagation models are being designed nowadays based on actual mathematical observations [42], [43] as a function of antenna height, frequency, distance, and different factors to obtain the maximum outcome [44]. For mmwave 5G spectrum, Alpha-Beta-Gamma (ABG) model, Close in (CI) free space reference distance and CI model with a weighted frequency called path loss exponent (CIF) model, provide comparable prediction accuracy with indoor propagation models by using large datasets of experimental results [45], [46]. At the same time, according to [47], the Log-Normal Shadowing path loss model shows that a negative cross-correlation exists between channels' ms delay spread and shadow fading. A comparison between CI and the Floating Intercept (FI) method revealed that the standard deviation is similar for all environments and layouts [48]–[50]. The total path loss is calculated by adding up all elevation pointing angle combinations and the received power of each unique azimuth [49]. Whereas for the same omnidirectional path, the model can be minimized to 1.1 – 1.3 in a 1 m closed free space within the referencing area [50], indicating great improvements for the propagation through the free space. The frequency of propagation and antenna height [51], [52] also plays a vital role in indoor modeling for path loss. Different multifrequency and single frequency path loss models for indoor environments are discussed in [51].

The findings of the study [52] show that a greater range of locations can be covered by increasing the transmitter height of the base station in densely populated urban areas, but the improvements still lack coverage in large regions past 300m [53]. In [54], characteristics for the propagation of mmwave of 5G channels are discussed. The time-dispersion parameters and PL for an outdoor environment are estimated at frequencies ranging from 10 to 40 GHz [55], [56]. Multi-frequency analysis in [57], [58] shows that based on its simplicity, physical stability, and low path loss for outdoor environments, the CI model is more suitable. These models are further compared for future 5G systems in [59]. According to [60], the CI model is far more reliable and robust in outdoor environments than the ABG model. Researchers have concluded that around 60 GHz it is possible to establish a good communication link that can hold up to 77 m in a hilly area outdoors and 134 m in an indoor environment [61]. It has also been reported that CI model path losses are far lower than those of other models [62].

The shadow factors in the models proposed in [63] show more advantageous results as compared with path loss models that use close-in reference. Especially, the different models presented in the research dictate that the shadow factor is reduced in different cities, approximately by 1 – 6 dB. While covering larger areas, the results in [64] show that ABG and CI models do not differ much in performance outcomes when real-life data is used. While the ABG model requires three virtually established parameters and offers a fraction of a dB smaller shadow factor, the CI model offers one physically-based parameter and simplicity along with providing a more conservative path loss estimate at long distances. In [65], the characteristics of the channel propagation are analyzed at 28 GHz using a 3D-ray-tracing simulation. Furthermore, for street-canyon environments, path loss models with dual slopes are proposed. According to different

measurements conducted at 28 GHz, the effective cell coverage area for the simulation was considered 220 m [66], which also agrees closely with further measurements conducted in [33]. Based on these results, it is concluded that roughly for the same coverage area, the deployed sites with random beamforming will be increased three times for 5G networks. The preliminary findings presented in [67] can help revise the channel models designed for frequencies below 6 GHz to extend their capabilities extensively. Table II further summarizes the comparison between different models in indoor environments and what type of antenna has been used for testing. It gives an overview of the different models that are suggested to be used in different environments for specific frequency ranges for 5G.

The main issue in the next-generation network (5G) is to ensure high-speed data to the users all the time. Many solutions will be required to achieve this goal, e.g., extreme densification of networks (small cells), heterogeneous networks, increased bandwidth and spectral efficiency of massive Multiple Input Multiple Output (MIMO) systems, interference management, and optimized resource allocation.

Table II. Proposed radio propagation model for indoor 5G

Path Loss Model	Frequency (GHz)	Antenna	Range (m)	Test Environment	Location
ABG model, CIF model [40]	2 – 73	Directional Steerable Horn Antenna	4 – 1238	Indoor office and shopping mall scenarios	USA and Denmark
Log-Normal Shadow Loss model [47]	40	High Directional Horn Antenna	52	Corridor (LOS) and Hall with both LOS and NOS measurement	Malaysia
CI model, FI model [68]	60	Highly Directional Antenna	27	Corridor and Classrooms on the 9th floor	USA
Omnidirectional CF model, FI model [68]	28 and 73	High Directional 27 dBi and 24.5 dBi gain horn antennas	30 – 200	Downtown Manhattan	USA
Directional and Omnidirectional CI model [50]	14 and 22	Highly Directional 15 dBi horn antennas	3.9 – 45.9	Modern office building with cubicles	South Africa
Large scale path loss model with dual-slope [69]	28 and 73	Wideband directional pyramidal horn antennas	2 – 24	Indoor Corridor environment on 5th floor	USA
Single Frequency CI, FI model, and Multi-frequency CI, ABG, CIF model [51]	28 and 73	Widebeam TX and RX antennas indoor	3.9 – 45.9	Indoor office environment	USA

This paper focuses on the utilization of wideband unlicensed frequency ranges for femtocells below 6 GHz and licensed bands above 6 GHz in femtocells to increase the data rates. However, a highly accurate analysis related to the path loss is needed for the resolution of this problem. In indoor environments, finding out the exact path loss is a very complex task as indoor surroundings vary from building to building. The main highlights of this study are as follows:

- In-depth literature review of radio propagation models for indoor femtocells
- Identification of problems in currently available propagation models
- Numerical analysis of radio propagation models for below 6 GHz frequency band
- Numerical analysis of radio propagation models for above 6 GHz frequency band

The remainder of the paper is organized as: Section 2 discusses the radio propagation models below 6 GHz that are proposed for usage in unlicensed bands, while Section 3 describes radio propagation models above 6 GHz and in the mmwave spectrum of 5G. The results and comparative analysis are presented in Section 4. The paper is concluded in Section 5 along with future directions.

2. Radio Propagation Models below 6 GHz

2.1 Log-Distance Path Loss Model

This path loss model is a very simple and basic type of model for radio power loss estimation in different environments, which can be further expressed as the following equation [64], [70]:

$$\mathrm{PL\ (dB)} = \mathrm{PL\ (do)} + 10\mathrm{n}.\log\left(\frac{d}{d_0}\right) + X_\sigma \qquad (1)$$

In equation (1), 'n' represents the path loss exponent that describes the increasing rate of path loss distance and is dependent on surrounding, d_0 represents the reference distance; the distance between the receiver and transmitter is 'd' and X_σ is the normal random variable with zero mean describing the attenuation factor in dB. The detailed parameter values for this model are shown in Table III [70], while Figure 1 illustrates the different path losses for the log-distance path loss model for a distance of 20 m for 5.5 GHz. The analysis has been done in Matlab 2020b, running on an Intel Core i7-9700 CPU with 64 GB Ram.

Table III. Parameters for calculation of log-distance model

Environment	Path loss exponent (n)	Standard Deviation (X_σ)	Distance Tx-Rx 'd' (m)	Reference Distance (d_0)
Free space	2	3.2 dB for single floor	20	2
Urban Area	3.5			2
Shadowed urban	4.5			2
In-building LOS	1.7			2
In-building Obstruction	5			2
In-factory Obstruction	2.5			2

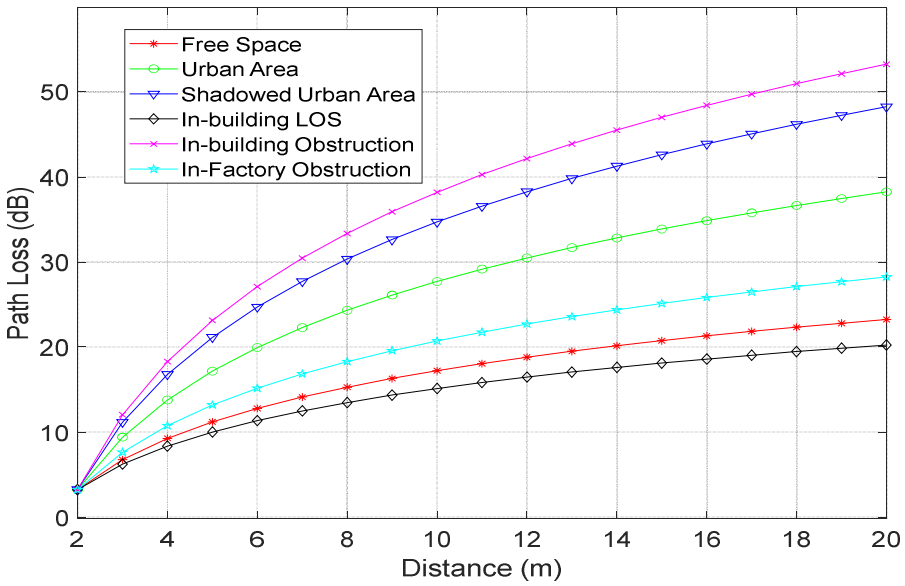

Figure 1. Path loss for log-distance model

2.2 Attenuation factor model

The attenuation factor model (AF) is a very compact model for the accurate calculation of propagation variations due to obstacles or the material type of the building. This indoor model provides path loss deviation and predicted values with a nearly 4 dB accuracy margin [71], while with the previous log-distance model the result is close to 13 dB for multiple buildings. Different parameters for a single floor for the AF model with a frequency of 5.5 GHz are shown in Table IV [70].

Table IV. Single floor parameters for the AF model at 5.5 GHz

Environment	n_{SF} (dB)	Distance (m)	Reference Distance (d_0), (m)	FAF (dB)	PAF (dB)
Grocery store	1.8	20	2	13	Foil insulation + ceiling duct 3.9+7=10.9
Office soft partition	2.4				Concrete wall + light textile 13+4=17
Office hard partition	3.0				Fade of 90^0+ Machinery 11+10=21
Metalworking	3.3				Cardboard+ Aluminum sheet 5+47=52

The AF model is given by the following Eqn. (2) [70]:

$$\mathrm{PL(d)\ [dB]} = \mathrm{PL}\,(d_0)\ \mathrm{[dB]} + 10n_{SF}\log\left(\frac{d}{d_0}\right) + \mathrm{FAF\ [dB]} + \sum PAF\ \mathrm{[dB]} \qquad (2)$$

In equation (2), the specific floor attenuation factor is known as FAF, n_{SF} is the path loss exponent for the AF model for the same floor. Whereas, for the floor with partitions presented with some obstacles or materials in the same way is expressed by PAF. Adding up all these losses due to partition and other obstacles results in a measured value that makes it more accurate. Figure 2 shows the path loss for the AF model for a single floor based on different values of the insulation material used.

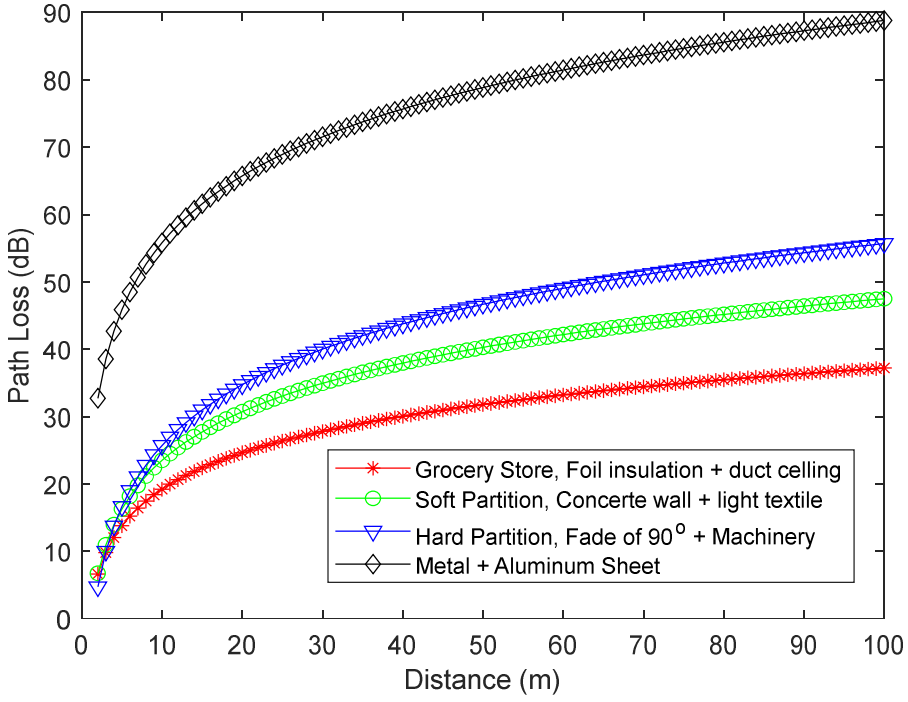

Figure 2. Attenuation Factor Model for the single floor scenario.

For multiple floors, the total path loss is obtained by considering the partition loss and integrating it with FAF. The exponent already having the effect of separating multiple floors may replace the attenuation factor for the floor. The path loss equation will be now as follows [70]:

$$\text{PL (d)[dB]} = \text{PL}\,(d_0) + 10n_{MF}\log\left(\frac{d}{d_0}\right) + \text{FAF [dB]} + \sum PAF\ \text{[dB]} \quad (3)$$

In equation (3), the multiple floors path loss exponent is n_{MF}. Table IV shows the values of n_{MF} (path loss exponent) for different buildings that are at multiple locations. It also shows that as the distance becomes larger, the path loss also increases. Table V [70] shows the value of parameters for the AF model for multiple floors at 5.5 GHz, whereas Figure 3 shows the value of the AF model for a different number of floors based on different parameters.

Table V. Parameters for the AF model considering multiple floors at 5.5 GHz

Environment	n_{MF} (dB)	Distance (m)	Reference Distance (d_0), (m)	FAF (dB)	PAF (dB)
Same floor	2.76	100	20	13	13+5=18 (concrete + cardboard)
One floor	4.19			14.6	14.6+5=19.6
Two floors	5.04			18.7	18.7+5=23.7
Three floors	5.22			24.4	24.4+5=29.4

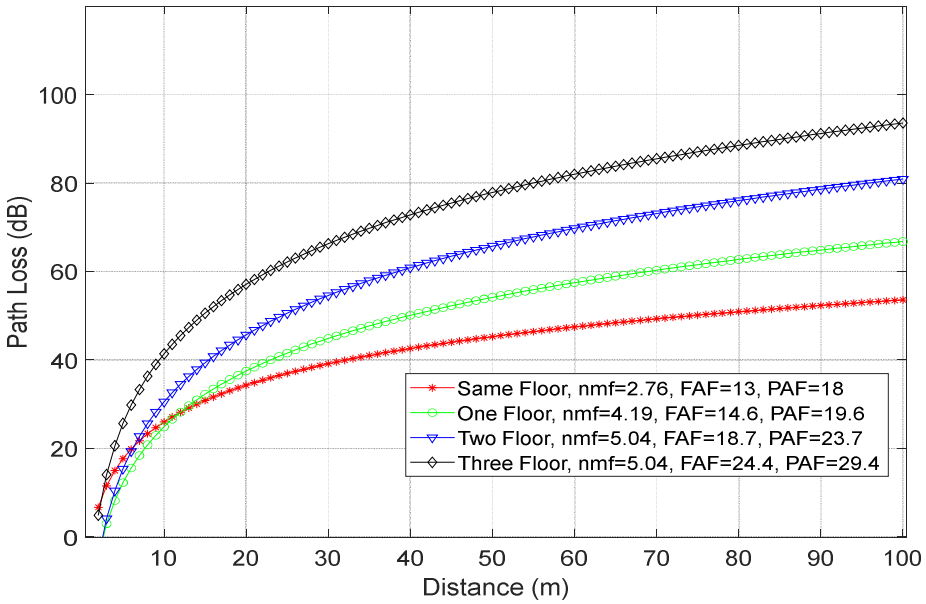

Figure 3. AF model path loss for different floor scenarios

3.3 ITU Model

ITU model is used to predict a signal loss for any enclosed area including partitions or walls. This model is best for frequencies in the range of 900 MHz to 5.5 GHz, but the model can also be used for frequencies falling in the broader range [72]. This model can cover up to three floors efficiently. The path loss for this model is defined as [72]:

$$PL = 20\,Log\,(f) + N\,Log\,(d) + Pf\,(n) - 28 \quad (4)$$

In Eqn. (4), the frequency is represented by f (MHz), distance is 'd', Pf(n) is the path loss factor. In Eqn. (4), N describes the attenuation of signal strength based on the distance between the

destination and source and the number of floors or obstacles. Table VI gives the different path loss coefficient values of N [73]. In addition, the path loss of the ITU model for different values of N and frequency is presented graphically in Figure 4.

Table VI. Path loss factor coefficient value for the ITU model

Frequency	Residential (N)	Office (N)	Reference Distance (d_0)	Commercial (N)
2.4 GHz	28	30	22	2.4 GHz
5.5 GHz	N/A	31	N/A	5.5 GHz

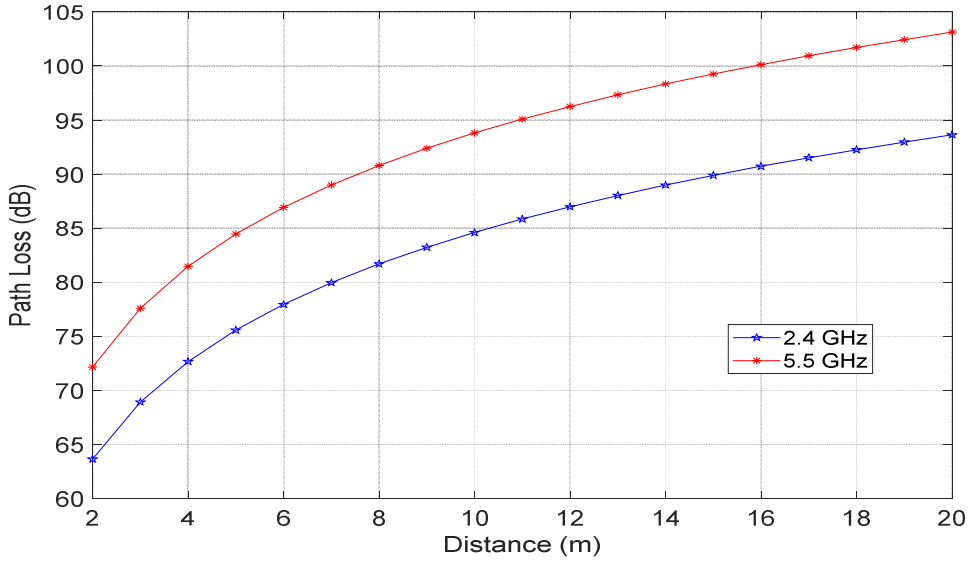

Figure 4. Path loss for ITU model for a single floor

The value of N for 2.4 GHz is 27 dB for the first, 35 dB for the second, and 40 dB for the third floor. The value of floor attenuation loss is empirical, depending on the number of floors present in the building or the environment; the different values are listed in Table VII [73].

Table VII. Floor attenuation loss factor pf(n) for the ITU model

Frequency	No of floors	Residential	Office	Commercial
2.4 GHz	1-3	4n	15+4(n-1)	6+3(n-1)
5.2 GHz	1	N/A	16	N/A

3.4 Keenan Motely Model

The Keenan Motley (KM) model presents one of the most precise, modified, and realistic calculations for radio propagation in an indoor environment. The path loss calculated using the KM model can be shown in the equation as [74]:

$$PL_{dB} = PL(d) + (N_W \,.\, \mathrm{W}) + n_F . L_F \quad (5)$$

In Eqn. (5), 'f' is the frequency (MHz), 'd' is the distance, the wall loss factor is 'W', where the number of walls in between the coverage area is represented by N_W , n_F is the number of floors and L_F is the corresponding attenuation factor. The attenuation values for concrete and plasterboard with the wall loss factor of 14 and 5 dB, respectively, for 2.4 GHz, but these values vary with the carrier frequency [71]. Table VIII shows the parameters for the KM model taking into account the distance

to be 30 m [71]; whereas Figure 5 describes the different path losses for the KM model concerning the distance for different frequencies.

Table VIII. Wall loss due to concrete for Keenan-Motley model

Carrier Frequency (GHz)	Number of walls (N_W)	Wall loss factor (W)
2.4	2	5
5.5		7

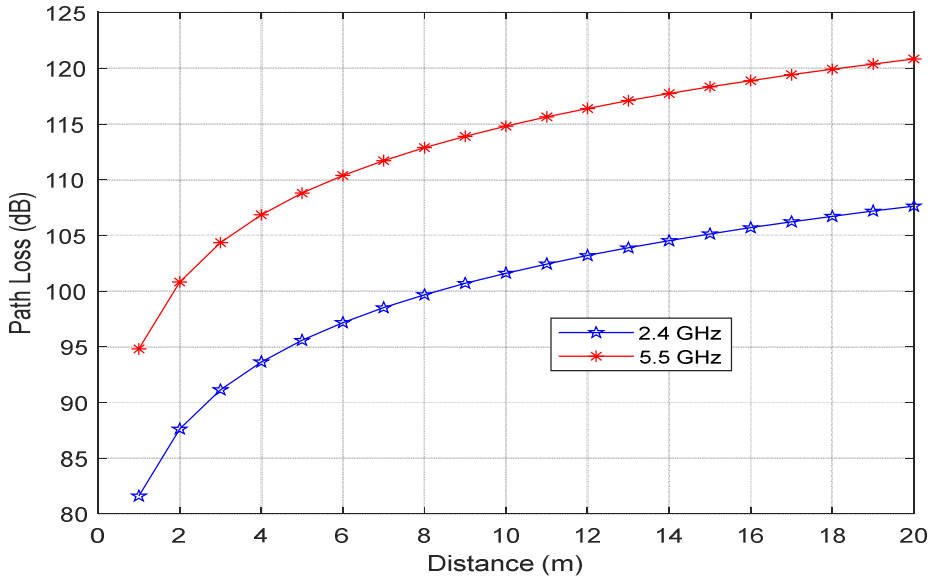

Figure 5. Keenan Motley model of path loss.

3.5 Joint Technical Committee (JTC) Model

The JTC model takes into account the signals passing through the windows of multiple floors as well for the calculation of the path loss. Thus, the JTC model can be described in the equation as [73]:

$$PL = A + L_f(n) + B\ log\ (d) + X \quad (6)$$

In Eqn. (6), the L_f(n) is the signal attenuation due to multiple floors and X is the log-normal distribution which describes the shadow fading for the signal, the gradient distance is 'B' and the attenuation distance is 'A'. Table IX lists the different values of parameters that are suggested for the JTC model in a given environment [75]. The only assumption taken for these parameters is that the receiver and transmitter are in the same building. Figure 6 illustrates the path loss for a single floor using the JTC model for different distances and Figure 7 describes the same for a two-floor building.

Table IX. Parameters for JTC Model

Environment	Residential	Office	Commercial
A (dB)	38	38	38
B	28	30	22
L_f(n) (dB)	4n	15+4 (n-1)	6+3 (n-1)
X	8	10	10

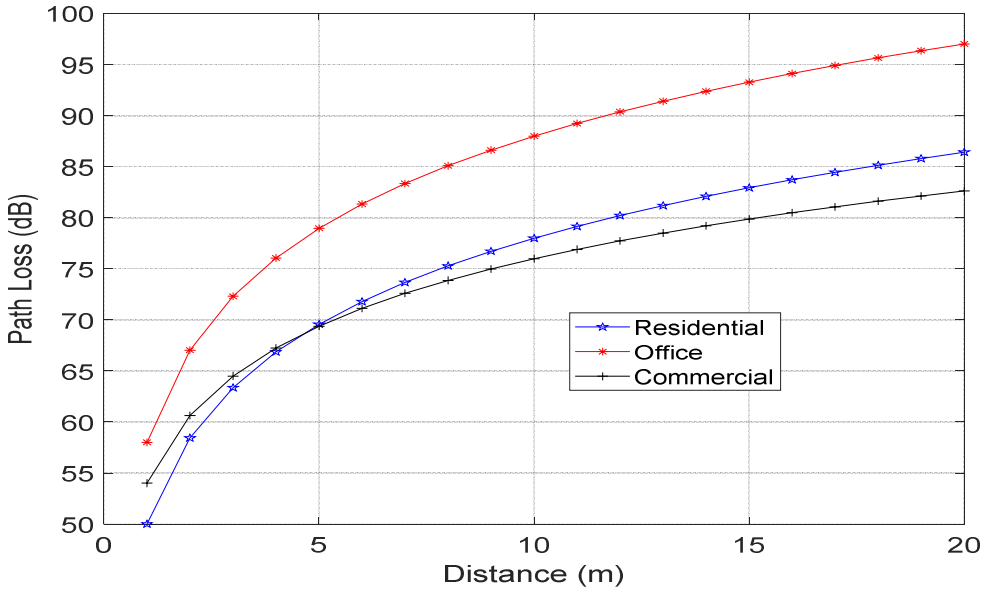

Figure 6. JTC model path loss for a single floor for 5.5 GHz

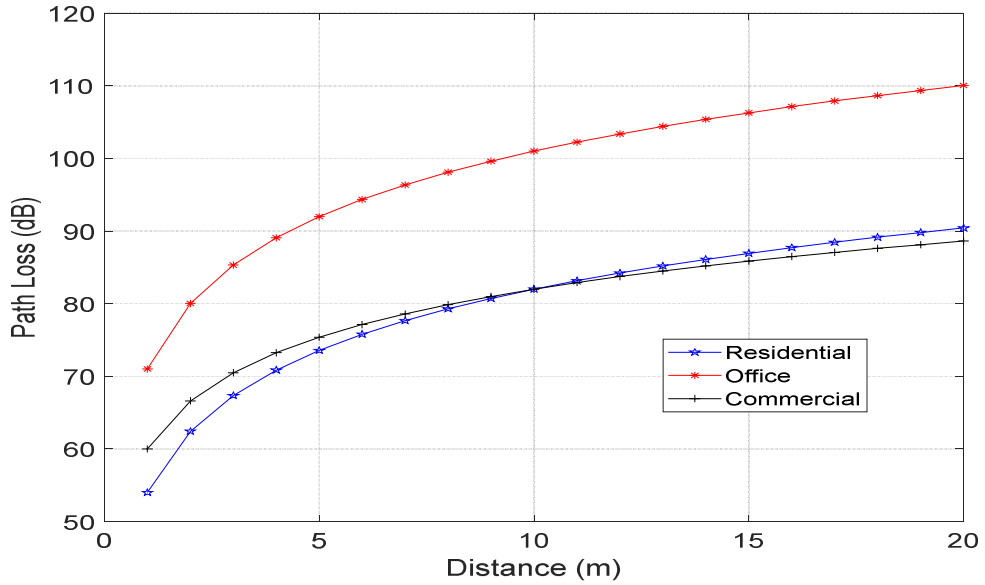

Figure 7. JTC model path loss for two floors for 5.5 GHz

3.6 Modified Keenan-Motely Model

This model considers building material as the most important factor for indoor path loss calculation [75]. The construction material attenuation model in equation form is

$$\mathrm{PL} = L_0 + 20\mathrm{Log}\,(\mathrm{d}) + \sum m_{type}\, w_{type}. \qquad (7)$$

We note that Eqn. (7) involves two new factors, m_{type} shows the number of partitions/walls and w_{type} is the loss in dB for that particular partition/wall. Table X shows the partition-dependent losses of the signal when fading on different wall types [71]. Figure 8 describes the path loss of different wall materials for this model.

Table X. Partition dependent losses for the modified Keenan-Motley model

The signal loss at 2.4 GHz	dB
Window in the brick wall	2
Metal frame, glass wall in the building	6
Wall of office	6
Metal door in office wall	6
Cinder wall	4
Metal door in the brick wall	12.4
The brick wall next to the metal door	3

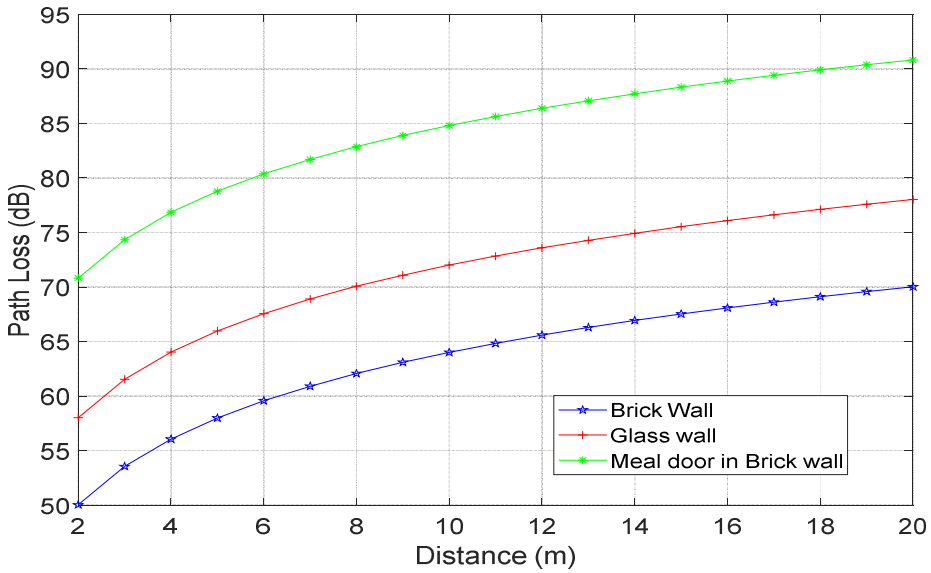

Figure 8. Modified Keenan-Motley model path loss

3. Radio Propagation Models above 6 GHz

3.1 A*lpha Beta Gamma model*

Alpha Beta Gamma (ABG) model contains distance and frequency factors to calculate path loss over a range of frequencies and can be used for both residential and industrial environments. The mathematical equation of the ABG model is given below in Eqn. (8) [27]:

$$\mathrm{PLABG}(f,d)[\mathrm{dB}] = 10\alpha\log10\ (d\ 1\ m) + \beta + 10\gamma\log10\ (f\ 1\ GHz) + \mathrm{X}^{\mathrm{ABG}}, \quad (8)$$

where PLABG (*f, d*) is indicating the path loss present in the propagation waves and can be measured in dB, the coefficient, which explains that with the increase in the distance between the receiver and transmitter the path loss will also increase is represented by α and γ shows that the path loss varies along with the variations in frequency. The distance between the receiver and transmitter is represented by d and is measured in meters, whereas the path loss floating offset is represented as β and the frequency used for carrying the radio waves is given by f and is measured in GHz and X^{ABG}, σ is the standard deviation explaining fluctuations of signals across the mean path loss over distance.

Path loss analysis for ABG model by varying coefficients α, β, and γ, where α, γ are path loss coefficients that depend on the distance and frequency while β is the optimization factor. Figures 9 and 10 show the path losses with distance for different values of α, β, and γ.

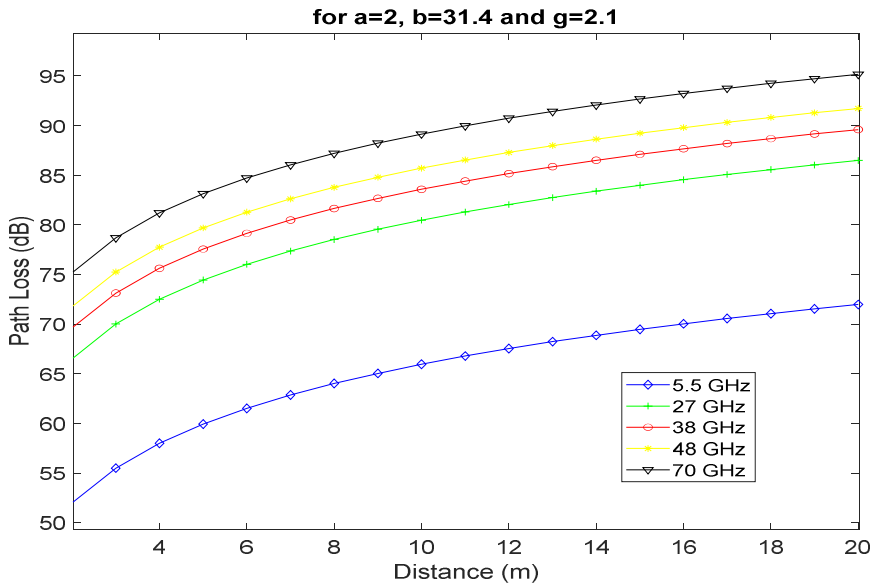

Figure 9. Path loss for ABG Model (α=2.1, β=31.4, γ=2.1)

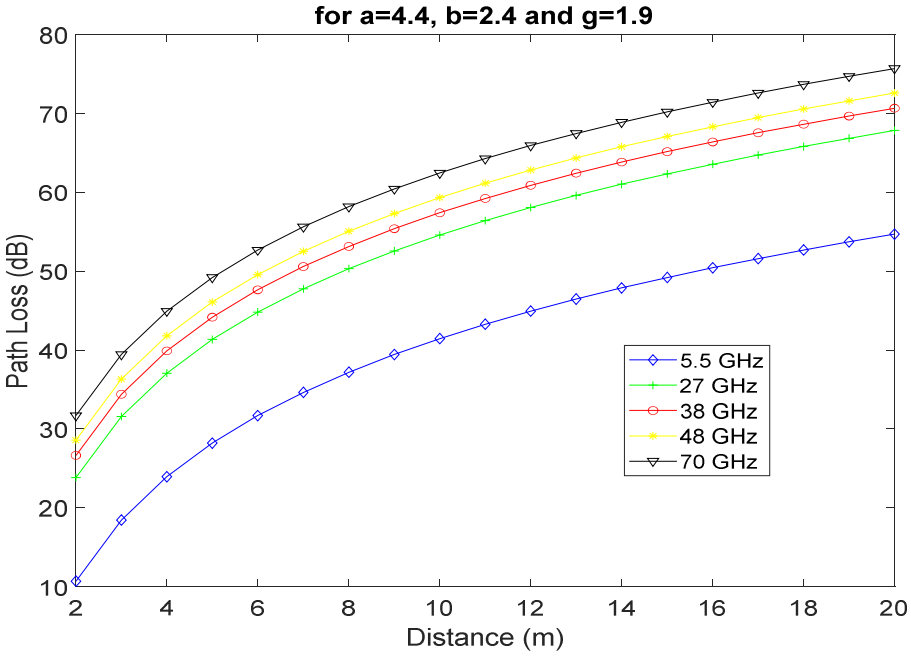

Figure 10. Path loss for ABG Model (α=4.4, β=2.4., γ=1.9)

3.2 Close in free space reference distance model (CIF)

The CIF reference distance model is an extension to the CI model and uses fewer parameters than ABG to calculate the path loss. The CIF model is also more efficient than the CI model; both models will be considered here.. The CIF model in Eqn. (10) further shows the details regarding the CIF model [48]. In Eqn. (10), *n* is the path loss exponent (PLE), *b* is the optimizing parameter, *d* is the 3D separation between transmitter and receiver, and FSPL indicates the free space path loss in dB at a separation distance of 1 m between transmitter and receiver. The equations for FSPL are given below in Eqn. 11 and Eqn. 12. Also, the path loss with respect to distance for the CIF model for different values of path loss exponents is given in Figure 11 and Figure 12.

$$PL^{CIF}(f,d)[dB] = FSP(f,1m)[dB] + 10n\left(1 + b\left(\frac{f \quad fo}{fo}\right)\right) log_{10}(d) X_{\sigma}^{CIF} \quad (9)$$

$$FSPL\,(f,1\,m)[dB] = 20log10\,(4\pi fc) \quad (10)$$

$$fo = \frac{\sum_{K=1}^{K} fkNk}{\sum_{K=1}^{K} Nk} \quad (11)$$

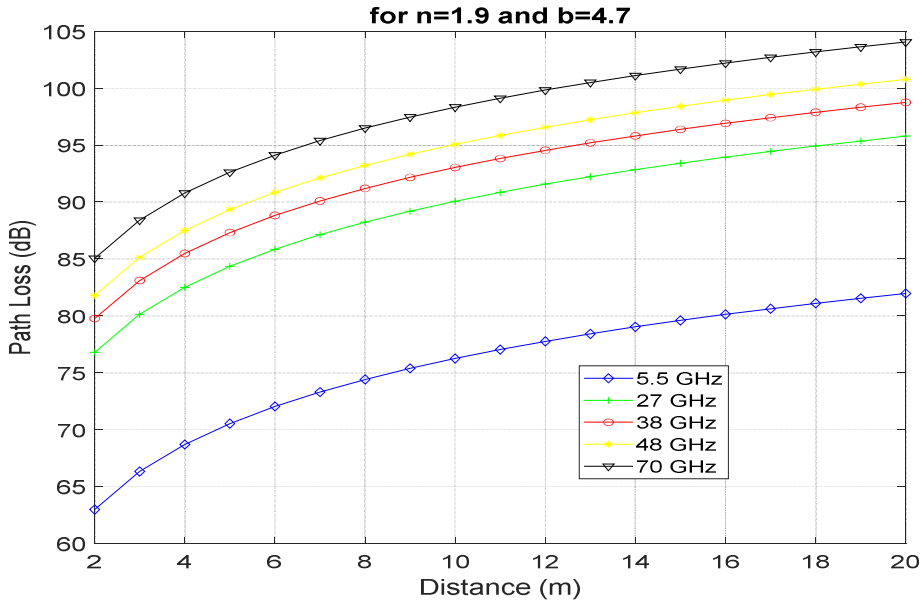

Figure 11. Path loss for CIF model (n=1.9, b=4.7).

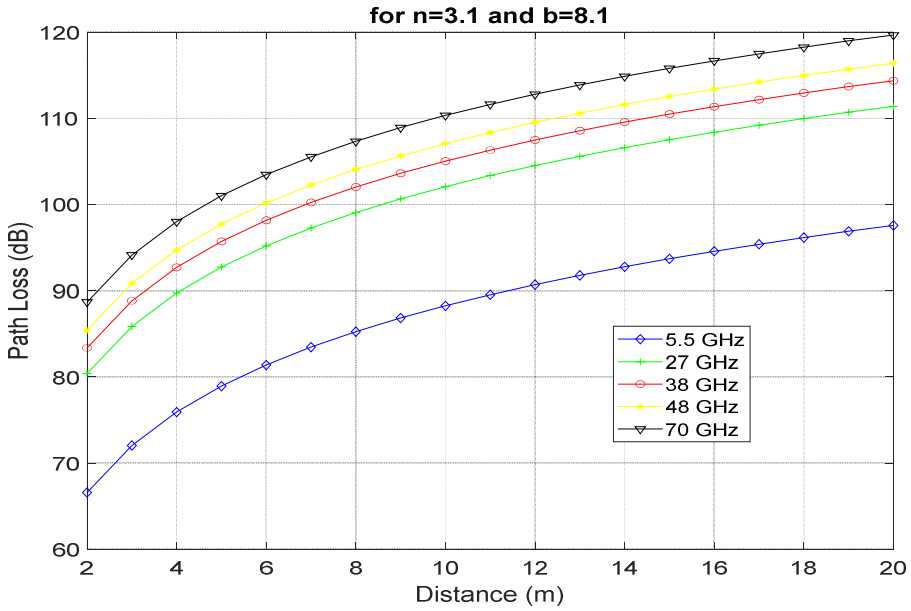

Figure 12. Path loss for CIF model (n=3.1, b=8.1).

Figure 13 depicts the path loss comparison for the NR-U 60 GHz unlicensed band in mmwave spectrum. The analysis of both ABG model and CIF model is shown here for two different set of parameters for both the models. This band in the mmwave is unlicensed and it has a proposed bandwidth of 7 GHz. It can also be utilized for very high data rates, applications like industrial control, monitoring and prognosis.

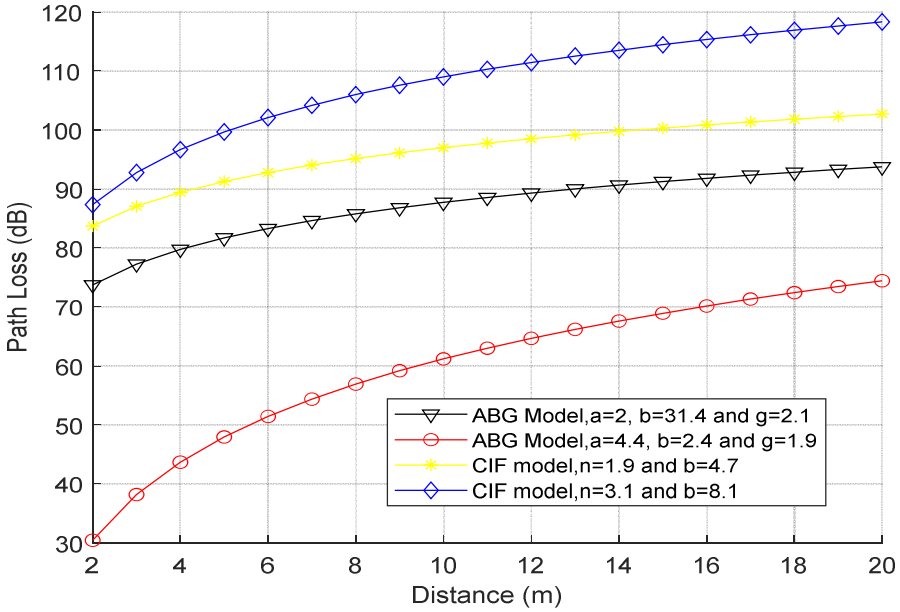

Figure 13. Path loss comparison for the 60 GHz unlicensed band

4. Results and Discussions

The main issue in the next-generation network (5G) is to ensure high-speed data to the users all the time. Many solutions will be required to achieve this goal, e.g., extreme densification of networks (small cells), heterogeneous networks, increased bandwidth and spectral efficiency of massive MIMO systems, interference management and optimized resource allocation. Therefore, femtocells will play a large role in 5G. Femtocell design is one of the most critical elements in providing high data rates and it is highly dependent on accurate path loss estimation.

The path loss depends on many variable factors, such as building material, the number of floors, attenuation, and shadowing. To calculate path losses for single and multiple buildings, several path loss models have been proposed. Each model has its unique characteristics and is designed for a specific environment. Some of the models need partition attenuation, whereas some need floor attenuation for measuring the exact values of path loss. For a specific building, the losses not only depend on the distance from the antenna but also the materials used inside the building, the floors in between the receiver and the transmitter, and the number of walls in between also plays a big role in the calculation of the path loss exponent 'n'. Some of the models can be extended to calculate the path loss in the same building with multiple floors, such an example of these models is the attenuation factor model and the JTC model.

5G will be using frequency in mmwave spectrum to provide higher data rates. It will also incorporate some unlicensed frequency bands that are shared by Wi-Fi technology for indoor femtocells. These 5G free unlicensed femtocells can be a good option for many industrial applications. The comparison of radio propagation models for below 6 GHz frequency is shown in Table XI. The log-distance path loss model discussed is usually good for a single floor, whereas the attenuation factor model is suitable for both multiple and single floors inside a building. Different models were discussed, and simulations were run in the indoor environment to calculate their respective path losses. The results shown and compared here are for a reference distance of 20 meters, but these results can be extended and calculated for 100 meters as well. The results indicate that the ITU model and Keenan-Motley model give the highest path loss in residential and industrial environments, respectively, while log-distance has the lowest path loss in both environments. These models are more suitable for low-frequency ranges (under 5 GHz).

Table XI. Comparison between path losses of different models under 6 GHz

Model name	Frequency (GHz)	Distance (m)	Path Loss PL (dB)	Environment	No. of Floors
Log – Distance	5.5	20	20 ─ 58	Residential/Industrial	1
Attenuation Factor (single floor)	5.5	20	43 ─ 98	Residential/Industrial	1
Attenuation Factor (multiple floors)	5.5	20	55 ─ 92	Residential/Industrial	3
ITU model	2.4 – 5.5	20	93 ─ 103	Residential	3
Keenan Motley model	2.4 – 5.5	20	105 - 121	Industrial	3
JTC model	5.5	20	83 ─ 96	Residential/Industrial	1
JTC model (Multi-floor)	5.5	20	88 ─ 110	Residential/Industrial	3
Modified Keenan Motely model	5.5	20	70 ─── 91	Industrial	3

As 5G will be using mmwave spectrum as well, therefore, the frequencies will be higher than 6 GHz and simply an extension of these models will not give significant results. The proposed models for frequencies higher than 6 GHz are compared in Table XII. The CIF model offers simplicity in the calculation of path loss as it only uses one parameter for calculation, whereas the ABG model uses three parameters. The path loss in the ABG model is directly dependent on α if its value is high, then path loss is also higher. Similarly, it is higher if the value of γ is equal to or larger than 2. In case of CIF model, the path loss is directly dependent on both the values of n and b. The value of n has a slightly greater effect on the overall path loss. The difference in path loss is very small in both models, but the ABG model shows more improved accuracy as compared with the CIF model based on its three parameters. Table 12 also shows the comparison of 60 GHz NR-U band. The path loss varies from 30 to 79 dBs for the ABG model and 82 to 118 form CIF model depending on the values of the parameters.

5. Conclusions and Future Work

This paper presents a comparison of different radio propagation models for indoor femtocells in view of the upcoming 5G technology. As 5G will incorporate many real-time services that require higher data rates and low latency. Therefore, 5G has the capability to provide feasible solutions for indoor users and capabilities for industrial monitoring and diagnostics using sensor-based networks and industrial IoT. Path loss analysis is mandatory for planning the cell size and it directly impacts the data rates. The large value of Signal to Noise Ratio (SNR) results in higher availability of data rate and vice versa. Due to this fact, the path loss analysis of the 5G femtocells is essential and discussed in detail in the paper.

Recently. The demand for higher data rates and good spectral efficiency has made indoor coverage more essential as the user is mostly located indoors. To overcome such challenges, femtocells are installed inside the indoor environment. The femtocell can cover the gaps and blank spots left by macrocells and increase the available bandwidth for the users. It is easier to handle FAPs transmission due to operation under a licensed spectrum or can share an unlicensed spectrum. Moreover, femtocells have auto-configuration and auto-optimization parameters. To adjust the transmission power of an internal device and for precision design, the most important factor is to measure the loss factor accurately.

Table XII. Comparison between path losses of different models above 6 GHz at 20 m.

Frequency (GHz)	α (dB)	β (dB)	γ (dB)	CIF model n (dB)	CIF model b (dB)	Path Loss (dB)
5.5 – 70	2	31.4	2.1	1.9	4.7	AGB = 73 -94 CIF = 82 - 104
5.5 – 70	2.6	24	1.6	2	2.9	AGB = 24 - 42 CIF = 84 - 105
5.5 – 70	2.8	11.4	2.3	2	4.6	AGB = 82 - 107 CIF = 84 - 106
5.5 – 70	3.3	17.6	2.0	2.7	1.0	AGB = 66 - 88 CIF = 93 – 115
5.5 – 70	3.5	24.4	1.9	2.8	8.3	AGB = 65 - 85 CIF = 94 - 116
5.5 – 70	4.4	2.4	1.9	3.1	8.1	AGB = 54 -75 CIF = 55 - 75
60	2	31.4	2.1	1.9	4.7	AGB = 30 -75 CIF = 82 - 103
60	4.4	2.4	1.9	3.1	8.1	AGB = 74 -95 CIF = 88 - 118

The analysis of the numerical results shows that the 5G femtocells are a viable solution for providing high data rates in 5G for both licensed and unlicensed bands. The accurate path loss estimation will help in designing better femtocells to solve the issue of coverage and quality of service. The comparative analysis of different indoor radio propagation models showed that the log-distance model has the lowest path loss between 20 to 58 dB which seems quite low, but the JTC and ITU models gives more realistic path loss around 90 and 100 dB, respectively, as they incorporate more parameters for unlicensed bands below 6 GHz. The ABG model and the CIF model give more or less the same values for path loss for frequencies above 6 GHz.

For future work, these models can be practically implemented and tested for accurate path loss analysis and some adjustments can be made in their mathematical models, if needed. The free band below 6 GHz unlicensed spectrum for the 5G network holds a good option for industrial sensor-based monitoring and diagnostic systems due to their high data rate and low latency potential. The possibility of unlicensed band of 60 GHz in the mmwave spectrum can also be explored. This range can be quite useful for high data rate indoor applications. The feasibility and path loss estimation of this network can also be verified. Another potential direction for future work could be the application of emerging machine learning techniques [76], [77] for enhanced analysis and prediction.

Funding: This research received no external funding.

Conflicts of Interest: The authors declare no conflict of interest.

References

[1] W. Lehr, F. Queder, and J. Haucap, "5G: A new future for Mobile Network Operators, or not?," *Telecomm. Policy*, vol. 45, no. 3, p. 102086, 2021, doi: 10.1016/j.telpol.2020.102086.

[2] ITU, "Guidelines for evaluation of radio interface technologies for IMT-2020," *Rep. ITU-R M.2412-0*, vol. 0, 2017.

[3] S. Ayyaz, U. Qamar, and R. Nawaz, "HCF-CRS: A Hybrid content based fuzzy conformal recommender system for providing recommendations with confidence," *PLoS One*, vol. 13,

no. 10, pp. 1–30, 2018, doi: 10.1371/journal.pone.0204849.

[4] M. R. Bhalla and A. V. Bhalla, "Generations of Mobile Wireless Technology: A Survey," *Int. J. Comput. Appl.*, vol. 5, no. 4, pp. 26–32, 2010, doi: 10.5120/905-1282.

[5] A. Maltsev, A. Pudeyev, A. Lomayev, and I. Bolotin, "Channel modeling in the next generation mmWave Wi-Fi: IEEE 802.11ay standard," *Eur. Wirel. Conf. 2016, EW 2016*, pp. 1–8, 2016.

[6] M. Cicioğlu, "Performance analysis of handover management in 5G small cells," *Comput. Stand. Interfaces*, vol. 75, no. July 2020, 2021, doi: 10.1016/j.csi.2020.103502.

[7] A. Çalhan and M. Cicioğlu, "Handover scheme for 5G small cell networks with non-orthogonal multiple access," *Comput. Networks*, vol. 183, 2020, doi: 10.1016/j.comnet.2020.107601.

[8] F. Boccardi, R. Heath, A. Lozano, T. L. Marzetta, and P. Popovski, "Five disruptive technology directions for 5G," *IEEE Commun. Mag.*, vol. 52, no. 2, pp. 74–80, 2014, doi: 10.1109/MCOM.2014.6736746.

[9] F. Luna, P. H. Zapata-Cano, J. C. González-Macías, and J. F. Valenzuela-Valdés, "Approaching the cell switch-off problem in 5G ultra-dense networks with dynamic multi-objective optimization," *Futur. Gener. Comput. Syst.*, vol. 110, pp. 876–891, 2020, doi: 10.1016/j.future.2019.10.005.

[10] ITU, "5G - Fifth Generation of mobile technologies." https://www.itu.int/en/mediacentre/backgrounders/Pages/5G-fifth-generation-of-mobile-technologies.aspx (accessed Aug. 08, 2020).

[11] W. S. Afifi, A. A. El-Moursy, M. Saad, S. M. Nassar, and H. M. El-Hennawy, "A novel scheduling technique for improving cell-edge performance in 4G/5G systems," *Ain Shams Eng. J.*, no. xxxx, 2020, doi: 10.1016/j.asej.2020.07.022.

[12] R. El Chall, B. Miscopein, and D. Kténas, "UNII-MAC protocol: Design and evaluation for 5G ultra-dense small cell networks operating in 5 GHz unlicensed spectrum," *Comput. Commun.*, vol. 126, no. February, pp. 11–27, 2018, doi: 10.1016/j.comcom.2018.04.005.

[13] M. Hawasli and S. A. Çolak, "Toward green 5G heterogeneous small-cell networks: power optimization using load balancing technique," *AEU - Int. J. Electron. Commun.*, vol. 82, no. June, pp. 474–485, 2017, doi: 10.1016/j.aeue.2017.09.012.

[14] N. Sabah, "4G TECHNOLOGY AND ITS APPLICATIONS," vol. VI, no. July, pp. 1–6, 2016.

[15] S. Sun, G. R. Maccartney, and T. S. Rappaport, "A novel millimeter-wave channel simulator and applications for 5G wireless communications," *IEEE Int. Conf. Commun.*, vol. 10, no. 1, pp. 1–7, 2017, doi: 10.1109/ICC.2017.7996792.

[16] S. Rangan, T. S. Rappaport, and E. Erkip, "Millimeter-wave cellular wireless networks: Potentials and challenges," *Proc. IEEE*, vol. 102, no. 3, pp. 366–385, 2014, doi: 10.1109/JPROC.2014.2299397.

[17] H. Taoka, S. Nagata, K. Takeda, Y. Kakishima, X. She, and K. Kusume, "MIMO and CoMP in LTE-Advanced," *NTT DOCOMO Tech. J.*, vol. 12, no. 2, pp. 20–28, 2010.

[18] B. Krenik, "4G Wireless technology: When will it happen? what does it offer?," *Proc. 2008 IEEE Asian Solid-State Circuits Conf. A-SSCC 2008*, pp. 141–144, 2008, doi: 10.1109/ASSCC.2008.4708715.

[19] S. Wangfi, W. Wang, and Y. Tan, "Internet cross-border service model based on 5G environment and cloud computing data platform," *Microprocess. Microsyst.*, no. November, p. 103520, 2020, doi: 10.1016/j.micpro.2020.103520.

[20] E. Dahlman, S. Parkvall, and J. Sköld, *4G LTE/LTE-advanced for Mobile Broadband*. .

[21] A. B. Saleh, Ö. Bulakci, S. Redana, B. Raaf, and J. Hämäläinen, "Enhancing LTE-advanced relay deployments via biasing in cell selection and handover decision," *IEEE Int. Symp. Pers. Indoor Mob. Radio Commun. PIMRC*, pp. 2277–2281, 2010, doi: 10.1109/PIMRC.2010.5671694.

[22] Jerry Sydir, "IEEE 802.16 Broadband Wireless Access Working Group - Harmonized Contribution on 802.16j (Mobile Multihop Relay) Usage Models," *IEEE 802.16 j Work. Gr. Doc. IEEE 802.16 j-06/015*, pp. 1–12, 2006.

[23] Z. Li, S. Guo, W. Li, S. Lu, D. Chen, and V. C. M. Leung, "A particle swarm optimization algorithm for resource allocation in femtocell networks," *IEEE Wirel. Commun. Netw. Conf. WCNC*, pp. 1212–1217, 2012, doi: 10.1109/WCNC.2012.6213962.

[24] R. Bajracharya, R. Shrestha, and H. Jung, "Future is unlicensed: Private 5g unlicensed network for connecting industries of future," *Sensors (Switzerland)*, vol. 20, no. 10, pp. 1–18, 2020, doi: 10.3390/s20102774.

[25] F. Zavoda, "State of the art sensors suitable for distribution automation application," CEATI Report No. T074700-5139, 2009.

[26] H. Claussen, L. T. W. Ho, and L. G. Samuel, "Self-optimization of coverage for femtocell deployments," *7th Annu. Wirel. Telecommun. Symp. WTS 2008*, pp. 278–285, 2008, doi: 10.1109/WTS.2008.4547576.

[27] S. Barbarossa, S. Sardellitti, A. Carfagna, and P. Vecchiarelli, "Decentralized interference management in femtocells: A game-theoretic approach," *2010 Proc. 5th Int. Conf. Cogn. Radio Oriented Wirel. Networks Commun. CROWNCom 2010*, pp. 1–5, 2010, doi: 10.4108/ICST.CROWNCOM2010.9276.

[28] R. K. Saha, "Realization of licensed/unlicensed spectrum sharing using EICIC in indoor small cells for high spectral and energy efficiencies of 5G networks," *Energies*, vol. 12, no. 14, 2019,

doi: 10.3390/en12142828.

[29] M. Sadik, N. Akkari, and G. Aldabbagh, "SDN-based handover scheme for multi-tier LTE/Femto and D2D networks," *Comput. Networks*, vol. 142, pp. 142–153, 2018, doi: 10.1016/j.comnet.2018.06.004.

[30] M. Yavuz *et al.*, "Interference management and performance analysis of UMTS/HSPA+ femtocells," *IEEE Commun. Mag.*, 2009, doi: 10.1109/MCOM.2009.5277462.

[31] N. Shabbir, M. T. Sadiq, H. Kashif, and Rizwan Ullah, "Comparison of Radio Propagation Models for Long Term Evolution (LTE) Network," *Int. J. Next-Generation Networks*, vol. 3, no. 3, pp. 27–41, 2011, doi: 10.5121/ijngn.2011.3303.

[32] I. Benyahia, "A Survey of Ant Colony Optimization Algorithms for Telecommunication Networks," *Int. J. Appl. Metaheuristic Comput.*, vol. 3, no. 2, pp. 18–32, 2012, doi: 10.4018/jamc.2012040102.

[33] M. Morita, Y. Matsunaga, and K. Hamabe, "Adaptive power level setting of femtocell base stations for mitigating interference with macrocells," *IEEE Veh. Technol. Conf.*, pp. 1–5, 2010, doi: 10.1109/VETECF.2010.5594572.

[34] S. Parkvall *et al.*, "LTE-Advanced - Evolving LTE towards IMT-Advanced," *IEEE Veh. Technol. Conf.*, pp. 1–5, 2008, doi: 10.1109/VETECF.2008.313.

[35] Ö. Bulakci, S. Redana, B. Raaf, and J. Hämäläinen, "Performance enhancement in LTE-Advanced relay networks via relay site planning," *IEEE Veh. Technol. Conf.*, pp. 1–5, 2010, doi: 10.1109/VETECS.2010.5493978.

[36] A. Damnjanovic *et al.*, "A survey on 3GPP heterogeneous networks," *IEEE Wirel. Commun.*, vol. 18, no. 3, pp. 10–21, 2011, doi: 10.1109/MWC.2011.5876496.

[37] Y. Wang and K. I. Pedersen, "Performance analysis of enhanced inter-cell interference coordination in LTE-advanced heterogeneous networks," *IEEE Veh. Technol. Conf.*, pp. 1–5, 2012, doi: 10.1109/VETECS.2012.6240233.

[38] D. López-Pérez, I. Güvenç, G. De La Roche, M. Kountouris, T. Q. S. Quek, and J. Zhang, "Enhanced intercell interference coordination challenges in heterogeneous networks," *IEEE Wirel. Commun.*, vol. 18, no. 3, pp. 22–30, 2011, doi: 10.1109/MWC.2011.5876497.

[39] S. Sun *et al.*, "Propagation path loss models for 5G urban micro-and macro-cellular scenarios," *IEEE Veh. Technol. Conf.*, vol. 2016-July, pp. 1–6, 2016, doi: 10.1109/VTCSpring.2016.7504435.

[40] S. Sun *et al.*, "Investigation of Prediction Accuracy, Sensitivity, and Parameter Stability of Large-Scale Propagation Path Loss Models for 5G Wireless Communications," *IEEE Trans. Veh. Technol.*, vol. 65, no. 5, pp. 2843–2860, 2016, doi: 10.1109/TVT.2016.2543139.

[41] S. Jaeckel, L. Raschkowski, K. Borner, and L. Thiele, "QuaDRiGa: A 3-D multi-cell channel

model with time evolution for enabling virtual field trials," *IEEE Trans. Antennas Propag.*, vol. 62, no. 6, pp. 3242–3256, 2014, doi: 10.1109/TAP.2014.2310220.

[42] A. Fricke, "TG3e Channel Modelling Document (CMD)," 2016.

[43] Ken Hiraga, "TG3e Channel Modelling Document (CMD)," 2015.

[44] R. J. Weiler *et al.*, "Quasi-deterministic millimeter-wave channel models in MiWEBA," *Eurasip J. Wirel. Commun. Netw.*, vol. 2016, no. 1, 2016, doi: 10.1186/s13638-016-0568-6.

[45] A. M. Al-Samman, T. A. Rahman, M. H. Azmi, and M. N. Hindia, "Large-scale path loss models and time dispersion in an outdoor line-of-sight environment for 5G wireless communications," *AEU - Int. J. Electron. Commun.*, vol. 70, no. 11, pp. 1515–1521, 2016, doi: 10.1016/j.aeue.2016.09.009.

[46] S. Sun, G. R. MacCartney, and T. S. Rappaport, "Millimeter-wave distance-dependent large-scale propagation measurements and path loss models for outdoor and indoor 5G systems," *2016 10th Eur. Conf. Antennas Propagation, EuCAP 2016*, pp. 1–5, 2016, doi: 10.1109/EuCAP.2016.7481506.

[47] A. M. Al-Samman, T. A. Rahman, M. H. Azmi, A. Sharaf, Y. Yamada, and A. Alhammadi, "Path loss model in indoor environment at 40 GHz for 5G wireless network," *Proc. - 2018 IEEE 14th Int. Colloq. Signal Process. its Appl. CSPA 2018*, no. March, pp. 7–12, 2018, doi: 10.1109/CSPA.2018.8368676.

[48] T. S. Rappaport, J. N. Murdock, and F. Gutierrez, "State of the art in 60-GHz integrated circuits and systems for wireless communications," *Proc. IEEE*, vol. 99, no. 8, pp. 1390–1436, 2011, doi: 10.1109/JPROC.2011.2143650.

[49] S. Deng, M. K. Samimi, and T. S. Rappaport, "28 GHz and 73 GHz millimeter-wave indoor propagation measurements and path loss models," *2015 IEEE Int. Conf. Commun. Work. ICCW 2015*, pp. 1244–1250, 2015, doi: 10.1109/ICCW.2015.7247348.

[50] N. O. Oyie and T. J. O. Afullo, "Measurements and Analysis of Large-Scale Path Loss Model at 14 and 22 GHz in Indoor Corridor," *IEEE Access*, vol. 6, pp. 17205–17214, 2018, doi: 10.1109/ACCESS.2018.2802038.

[51] T. S. Rappaport, F. Gutierrez, E. Ben-Dor, J. N. Murdock, Y. Qiao, and J. I. Tamir, "Broadband millimeter-wave propagation measurements and models using adaptive-beam antennas for outdoor Urban cellular communications," *IEEE Trans. Antennas Propag.*, vol. 61, no. 4, pp. 1850–1859, 2013, doi: 10.1109/TAP.2012.2235056.

[52] X. Zhao, S. Li, Q. Wang, M. Wang, S. Sun, and W. Hong, "Channel Measurements, Modeling, Simulation and Validation at 32 GHz in Outdoor Microcells for 5G Radio Systems," *IEEE Access*, vol. 5, pp. 1062–1072, 2017, doi: 10.1109/ACCESS.2017.2650261.

[53] A. M. Al-Samman, T. Abd Rahman, and M. H. Azmi, "Indoor corridor wideband radio

propagation measurements and channel models for 5G millimeter wave wireless communications at 19 GHz, 28 GHz, and 38 GHz Bands," *Wirel. Commun. Mob. Comput.*, vol. 2018, 2018, doi: 10.1155/2018/6369517.

[54] F. Al-Ogaili and R. M. Shubair, "Millimeter-wave mobile communications for 5G: Challenges and opportunities," *2016 IEEE Antennas Propag. Soc. Int. Symp. APSURSI 2016 - Proc.*, pp. 1003–1004, 2016, doi: 10.1109/APS.2016.7696210.

[55] R. J. Chandan Kumar Jha, "Literature Survey on Various Outdoor Propagation Model for Fixed Wireless Network," *Int. J. Sci. Res.*, vol. 3, no. 8, pp. 1601–1604, 2014.

[56] S. Stavrou, "Factors influencing outdoor to indoor radio wave propagation," pp. 581–585, 2005, doi: 10.1049/cp:20030142.

[57] G. R. Maccartney, T. S. Rappaport, M. K. Samimi, and S. Sun, "Millimeter-Wave Omnidirectional Path Loss Data for Small Cell 5G Channel Modeling," *IEEE Access*, vol. 3, pp. 1573–1580, 2015, doi: 10.1109/ACCESS.2015.2465848.

[58] S. Piersanti, L. A. Annoni, and D. Cassioli, "Millimeter waves channel measurements and path loss models," *IEEE Int. Conf. Commun.*, pp. 4552–4556, 2012, doi: 10.1109/ICC.2012.6363950.

[59] T. A. Thomas *et al.*, "A prediction study of path loss models from 2-73.5 GHz in an urban-macro environment," *IEEE Veh. Technol. Conf.*, vol. 2016-July, 2016, doi: 10.1109/VTCSpring.2016.7504094.

[60] A. I. Sulyman, A. Alwarafy, H. E. Seleem, K. Humadi, and A. Alsanie, "Path loss channel models for 5G cellular communications in Riyadh city at 60 GHz," *2016 IEEE Int. Conf. Commun. ICC 2016*, pp. 1–6, 2016, doi: 10.1109/ICC.2016.7510953.

[61] A. M. Al-Samman, M. N. Hindia, and T. A. Rahman, "Path loss model in outdoor environment at 32 GHz for 5G system," *2016 IEEE 3rd Int. Symp. Telecommun. Technol. ISTT 2016*, pp. 9–13, 2017, doi: 10.1109/ISTT.2016.7918076.

[62] S. Sun, T. A. Thomas, T. S. Rappaport, H. Nguyen, I. Z. Kovacs, and I. Rodriguez, "Path loss, shadow fading, and line-of-sight probability models for 5G urban macro-cellular scenarios," *2015 IEEE Globecom Work. GC Wkshps 2015 - Proc.*, 2015, doi: 10.1109/GLOCOMW.2015.7414036.

[63] G. R. Maccartney, J. Zhang, S. Nie, and T. S. Rappaport, "Path loss models for 5G millimeter wave propagation channels in urban microcells," *GLOBECOM - IEEE Glob. Telecommun. Conf.*, pp. 3948–3953, 2013, doi: 10.1109/GLOCOM.2013.6831690.

[64] S. Hur *et al.*, "Proposal on millimeter-wave channel modeling for 5G cellular system," *IEEE J. Sel. Top. Signal Process.*, vol. 10, no. 3, pp. 454–469, 2016, doi: 10.1109/JSTSP.2016.2527364.

[65] A. Sulyman, A. Nassar, M. Samimi, G. Maccartney, T. Rappaport, and A. Alsanie, "Radio propagation path loss models for 5G cellular networks in the 28 GHZ and 38 GHZ millimeter-

wave bands," *IEEE Commun. Mag.*, vol. 52, no. 9, pp. 78–86, 2014, doi: 10.1109/MCOM.2014.6894456.

[66] K. Haneda *et al.*, "5G 3GPP-like channel models for outdoor urban microcellular and macrocellular environments," *IEEE Veh. Technol. Conf.*, vol. 2016-July, 2016, doi: 10.1109/VTCSpring.2016.7503971.

[67] T. S. Rappaport *et al.*, "Millimeter wave mobile communications for 5G cellular: It will work!," *IEEE Access*, vol. 1, pp. 335–349, 2013, doi: 10.1109/ACCESS.2013.2260813.

[68] G. R. Maccartney, M. K. Samimi, and T. S. Rappaport, "Omnidirectional path loss models in New York City at 28 GHz and 73 GHz," *IEEE Int. Symp. Pers. Indoor Mob. Radio Commun. PIMRC*, vol. 2014-June, pp. 227–231, 2014, doi: 10.1109/PIMRC.2014.7136165.

[69] G. R. MacCartney, T. S. Rappaport, S. Sun, and S. Deng, "Indoor office wideband millimeter-wave propagation measurements and channel models at 28 and 73 GHz for Ultra-Dense 5G Wireless Networks," *IEEE Access*, vol. 3, pp. 2388–2424, 2015, doi: 10.1109/ACCESS.2015.2486778.

[70] T. S. Rappaport, *Wireless Communications: Principles and Practice*, 2nd ed. Prentice Hall, 2002.

[71] Y. A. O. Lu, "Propagation Modeling and Performance Evaluation in an Atrium Building," 2014.

[72] R. I.-R. P.1238, "Propagation Data and Prediction Models for the Planning of Indoor Radiocommunication Systems and Radio Local Area Networks in the Frequency Range 900 MHz to 100 GHz," 1997.

[73] S. Cebula *et al.*, "Empirical channel model for 2.4 GHz ieee 802.11 wlan," *Proc. 2011 Int. Conf. Wirel. Networks*, 2011.

[74] A. G. M. Lima and L. F. Menezes, "Motley-keenan model adjusted to the thickness of the Wall," *SBMO/IEEE MTT-S Int. Microw. Optoelectron. Conf. Proc.*, pp. 180–182, 2005, doi: 10.1109/IMOC.2005.1580040.

[75] S. Hosseinzadeh, H. Larijani, and K. Curtis, "An enhanced modified multi wall propagation model," *GIoTS 2017 - Glob. Internet Things Summit, Proc.*, pp. 56–59, 2017, doi: 10.1109/GIOTS.2017.8016211.

[76] S. U. Hassan, M. Imran, S. Iqbal, N. R. Aljohani, and R. Nawaz, "Deep context of citations using machine-learning models in scholarly full-text articles," *Scientometrics*, vol. 117, no. 3, pp. 1645–1662, 2018, doi: 10.1007/s11192-018-2944-y.

[77] R. Yunus *et al.*, "A Framework to Estimate the Nutritional Value of Food in Real Time Using Deep Learning Techniques," *IEEE Access*, vol. 7, pp. 2643–2652, 2019, doi: 10.1109/ACCESS.2018.2879117.